Biophysical Journal, Volume 97

**Supporting Material**

# Biophysics and Structure of the Patch and the Gigaseal

Thomas M. Suchyna, Vladislav S. Markin, and Frederick Sachs

# Methods

**Cell cultures:** Primary (activated) adult rat astrocyte cultures were isolated from gelatin-sponge implants as previously described (1), and maintained in DMEM, 10% fetal bovine serum, and 1% penicillin/streptomycin. Mouse myotubes were prepared from primary cultures of myoblasts from the flexor digitorum brevis muscle of 4-8 week old mice as described in (2). Cells were maintained in DMEM/F-12 with 10% fetal bovine serum and 1% penicillin-streptomycin solution. HEK cells were maintained in DMEM, 10% fetal bovine serum, and 1% penicillin/streptomycin. All experiments were performed at room temperature in normal bath saline (140 mM NaCl, 10 mM HEPES, 5 mM KCl, 2 mM $CaCl_2$, 0.5 mM $MgCl_2$, 5 mM glucose).

**Electrophysiology:** An Axopatch 200B (Axon Instruments, CA, USA) was used for patch clamping, and data acquisition was controlled by Axon Instruments pClamp9 software via a Digidata 1322A acquisition system. All potentials (across the dome) are defined with respect to the extracellular surface. The potentials referred to during creep experiments are defined as the difference between the pipette and the bath since it is the seal, not the membrane that divides the pipette and bath. Borosilicate and soda-lime soft glass pipettes were pulled on a HEKA PIP 5 pipette puller (Digitimer, Hertfordshire, UK), painted with Sylgard 184 (Dow Corning Corp., Midland, MI, USA) and fire polished. The softening temperature of soda lime glass (~580-600$^{o}$C) and dielectric constant (~7.8) are similar to Corning 8161 glass (softening temperature 600$^{o}$C and dielectric constant 8.3) used in references (3;4). Some borosilicate electrodes were also fire polished next to a molten bead of soft glass to coat the tip as described in (3).

The resting membrane potential in astrocytes was ~ −50 mV as measured upon breaking into whole-cell mode. Pressure and suction were applied to the pipette by an HSPC-1 pressure clamp (ALA Scientific Instruments, NY, USA) controlled by pClamp software. Long pressure steps (>1 sec) produced a steady state creep of the dome edge requiring the flow of new membrane into the tip (5) or unfolding of membrane within the seal. We minimized the contribution of pressure induced creep to the patch geometry by using short (0.5 sec) pressure steps. Patches were generally formed with weak (~2-4 mmHg) suction. Off-line data analysis was performed with Clampfit and Origin 7.0.

Normal pipette saline contained (in mM): KCl 140, EGTA 5, MgCl2 2 and Hepes 10; pH 7.3, and pipette resistances ranged from 2-4 MΩ. The pipette salines used to investigate seal properties are defined in Results. Since $E_a$ was measured at the junction of the dome and the glass we only varied the pipette saline. However, since patch creep may be affected by the ionic composition through the entire seal, we used symmetrical ionic conditions for these measurements. Excised patches were perfused with a BPS-8 (ALA Scientific) perfusion system. Patch impedance was measured as previously described (2).

**Fluorescence and Video microscopy:** Patch motion was visualized with differential interference contrast optics on a Zeiss Axiovert 135 inverted microscope (Oberkochen, Germany). The patch dome was aligned perpendicular to the shear axis of the Wollaston prisms, and the pipette approached the coverslip at ~$15^o$ for cell-attached patches. For excised inside-out patches the pipette was pressed against the coverslip to bend the shank parallel with the glass surface. The imaging optics were a Zeiss 63× 1.4 NA oil immersion objective and a condenser made of a 40× 0.8 NA water immersion objective (6). Images were collected at 30 frames $s^{-1}$ with an iXon DV887 camera (Andor, CT, USA) mounted on a 4× magnifier. Patch motion was analyzed using the 'tracker' function in ImageJ (rsb.info.nih.gov/ij/) and corrected for the approach angle of the pipette when necessary.

GFP fusion proteins of TREK and TRPC6 were constructed and expressed in HEK and COS cells. Expression patterns were visualized with the Axiovert using a Dual-View DV-CC (Optical Insights, USA) image splitter to observe GFP fluorescence and DIC image at 650 nm λ simultaneously. The glycocalyx was stained by incubating cells for 1 hr in bath saline containing WGA conjugated to Oregon Green (Molecular Probes) and then washed 2X for 5 minutes in bath saline.

**Statistical analysis:** Statistical differences between $E_a$ values for the different conditions were evaluated with a two sided t-Test using at 5% significance level.

Reference List for Methods


1. Suchyna, T. M., J. H. Johnson, K. Hamer, J. F. Leykam, D. A. Gage, H. F. Clemo, C. M. Baumgarten, and F. Sachs. 2000. Identification of a peptide toxin from Grammostola spatulata spider venom that blocks cation-selective stretch-activated channels. *J. Gen. Physiol* 115:583-598.

2. Suchyna, T. M. and F. Sachs. 2007. Mechanosensitive channel properties and membrane mechanics in mouse dystrophic myotubes. *J. Physiol* 581:369-387.

3. Gil, Z., S. D. Silberberg, and K. L. Magleby. 1999. Voltage-induced membrane displacement in patch pipettes activates mechanosensitive channels. *Proc Natl. Acad. Sci U. S A* 96:14594-14599.

4. Gil, Z., K. L. Magleby, and S. D. Silberberg. 1999. Membrane-pipette interactions underlie delayed voltage activation of mechanosensitive channels in Xenopus oocytes. *Biophys. J.* 76:3118-3127.

5. Yeung, A. 1994. Mechanics of intermonolayer coupling in fluid surfactant bilayers. Univ. British Columbia.

6. Sokabe, M. and F. Sachs. 1990. The structure and dynamics of patch-clamped membranes: a study by differential interference microscopy. *Journal of Cell Biology* 111:599-606.

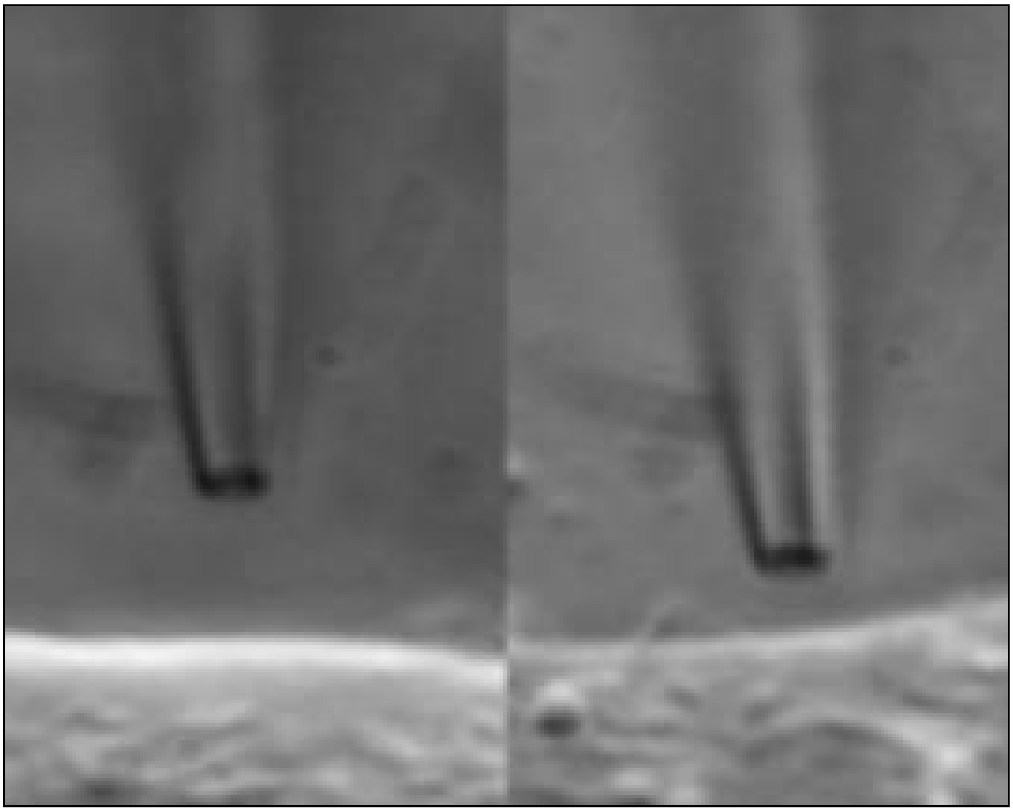

**Video S1** Videos showing patch formation on a myotube (slowly remodeling) and an HEK cell (actively remodeling). Video speed ~14X faster than real time. After the patch tip touches the surface ~-3 mmHg is applied to each pipette. During myotube patch formation the suction was briefly released several times during which time the patch was pulled back toward the cell. During patch formation on the HEK cell, the suction was reapplied several times near the end of the video to induce seal formation. In both patches, multiple bleb-like structures appeared before seal formation. Gigaseals for both patches did not form until the last 0.2 seconds of each video, when we observed a rapid stiffening of the patch dome. The patch shape from the HEK cell is much more irregular than that from the myotube.

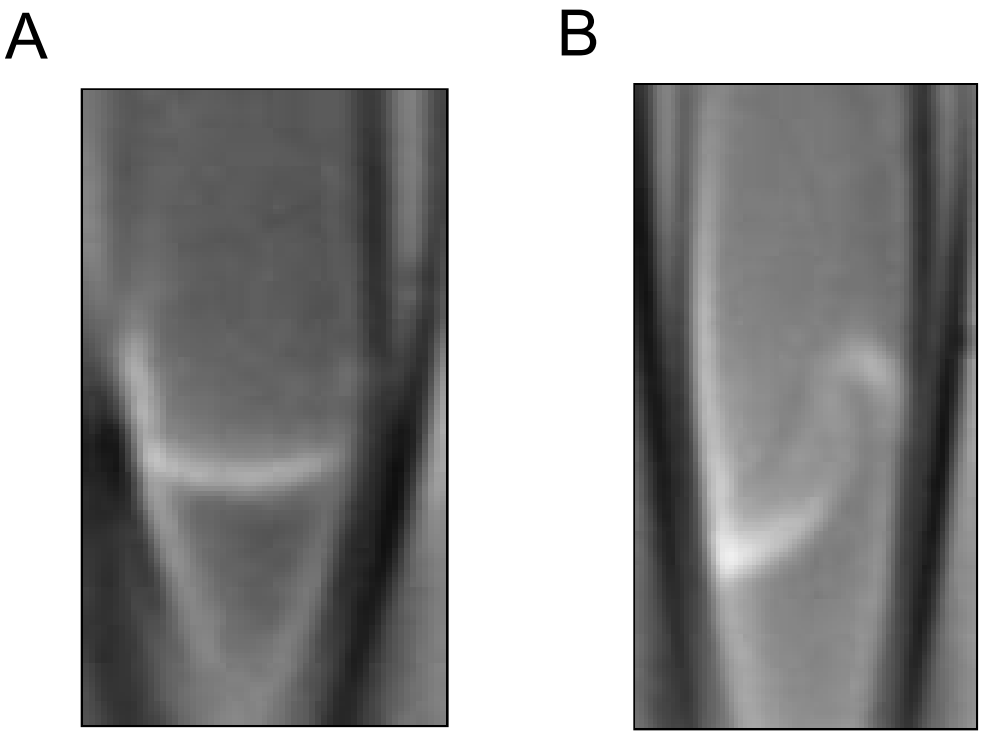


**Video S2** (A) Video of initial restructuring of an astrocyte patch as in Figure 2A. With 500 ms pressure steps, the membrane that is folded on the left peels apart and seals to the right side of the pipette. This form of "exercise" relaxes cytoskeletal stresses. (B) Initial restructuring of a COS patch in Figure 2B with pressure steps. A tether of membrane extending upward from the left side of the patch inflates during the first pressure step producing a bleb of membrane with a clear phase separation at the base of the bleb. When the patch was allowed to rest, the unusual initial geometry returned, and this shape change could be repeated several times showing that underlying cytoskeletal structure was quite robust.

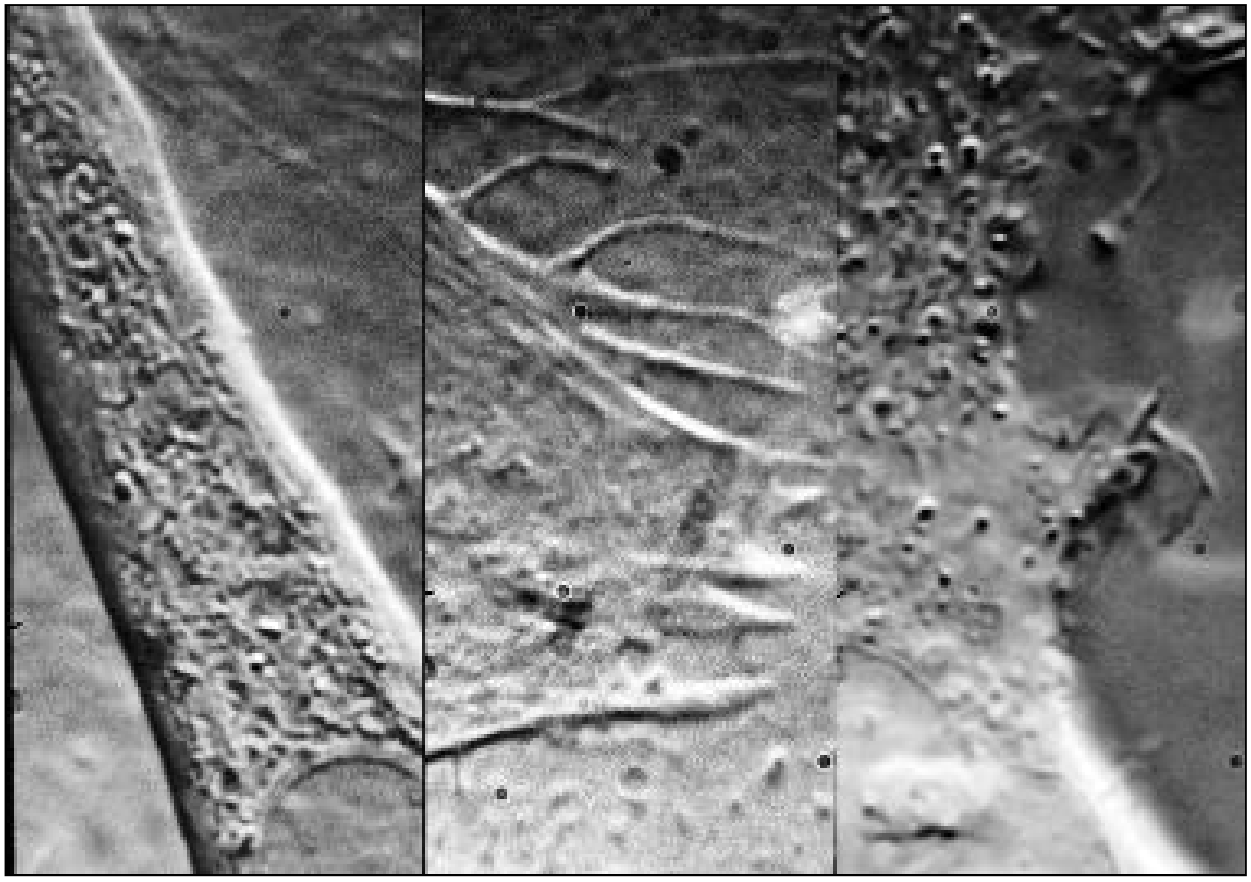

**Video S3** Time lapse video of three cell types (from left to right – myotube, astrocyte and HEK cell) with different rates of membrane remodeling (room temperature). The time lapse is 1 second in video = 2.5 min. The myotube cortex is relatively stiff and stable over many minutes. The HEK cortex is constantly remodeling and extending filipodia and lamellipodia. Cell types with greater remodeling rates have a more complex initial patch structure.

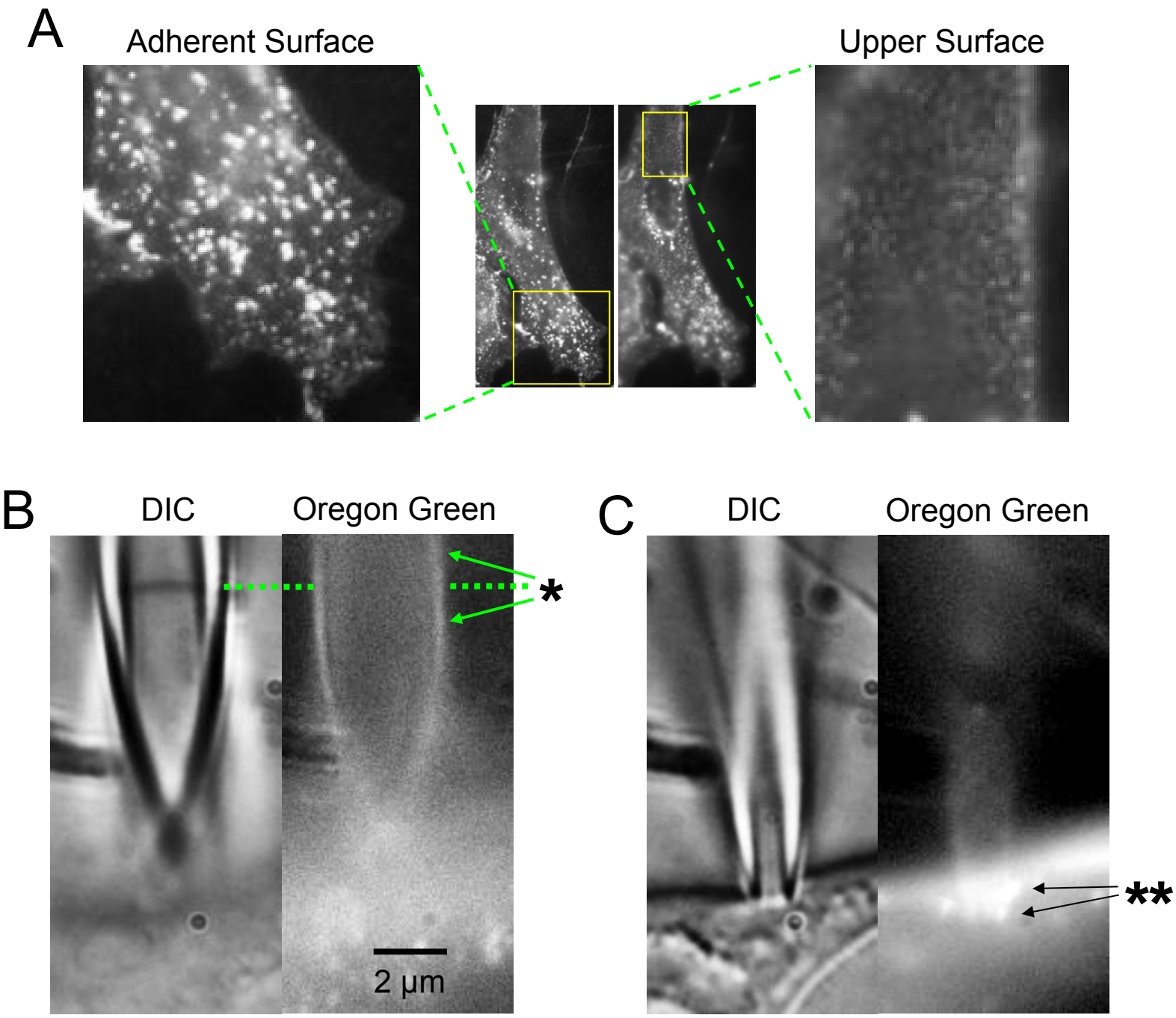


**Figure S4.** (A) Focusing on the adherent and upper surfaces of an astrocyte stained with Oregon Green labeled lectin (wheat germ agglutinin) shows that the distribution of glycocalyx differs between the surface in contact with the glass and the surface facing the media. This emphasizes that patches made from the upper surface do not represent the average cell properties. Patches made from labeled cells shows no fluorescence above background in the seal or the dome. (B) Shows that glycocalyx is excluded during patch formation. The fluorescence images were produced with long exposure times (3 seconds) and contrast enhancement to show the distribution of the weak lectin fluorescence on the cell surface. Contrast enhancement increased the appearance of autofluorescence of the glass which is why the outline of the pipette can be seen in the images, but notice that the intensities above and below the dome are equal (*) and hence not part of the patch. (C) Focusing on the pipette tip in contact with the cell shows an aggregation of labeled particles on the cell surface just outside the tip (**).

**Video S5.** Video at different focal depths showing that 500 mM KCl in the pipette creates a vesiculated patch structure. We couldn't form gigaseals with an ionic strength ≥500 mM, but we could induce blebs with high suction (-150 to -200 mmHg). These blebs would rapidly stiffen and fill the inside of the tip but not bind to the glass. In whole cells, hypertonicity induced a rapid (1-2 min) activation and translocation of ERM (ezrin/radixin/moesin) proteins to the cell surface (1) ERM proteins are involved in cytoskeletal remodeling, and their transport to the surface increases f-actin association with the cortex. The activation and translocation of ERMs is a phospholipase-C (PLC) dependent process where mechanical shrinkage of the membrane may be the stimulus. PLCs are activated by G-protein coupled receptors (GPCR), and recently it has been discovered that some GPCRs can be mechanically activated (2;3). This cytoskeletal reorganization may explain why high concentration saline increases the difficulty of making seals.

Reference List for Video S5


1. Rasmussen, M., R. T. Alexander, B. V. Darborg, N. Mobjerg, E. K. Hoffmann, A. Kapus, and S. F. Pedersen. 2008. Osmotic cell shrinkage activates ezrin/radixin/moesin (ERM) proteins: activation mechanisms and physiological implications. *American Journal of Physiology-Cell Physiology* 294:C197-C212.

2. Schnitzler, M. M. Y., U. Storch, S. Meibers, P. Nurwakagari, A. Breit, K. Essin, M. Gollasch, and T. Gudermann. 2008. G(q)-coupled receptors as mechanosensors mediating myogenic vasoconstriction. *Embo Journal* 27:3092-3103.

3. Voets, T. and B. Nilius. 2009. TRPCs, GPCRs and the Bayliss effect. *Embo Journal* 28:4-5.

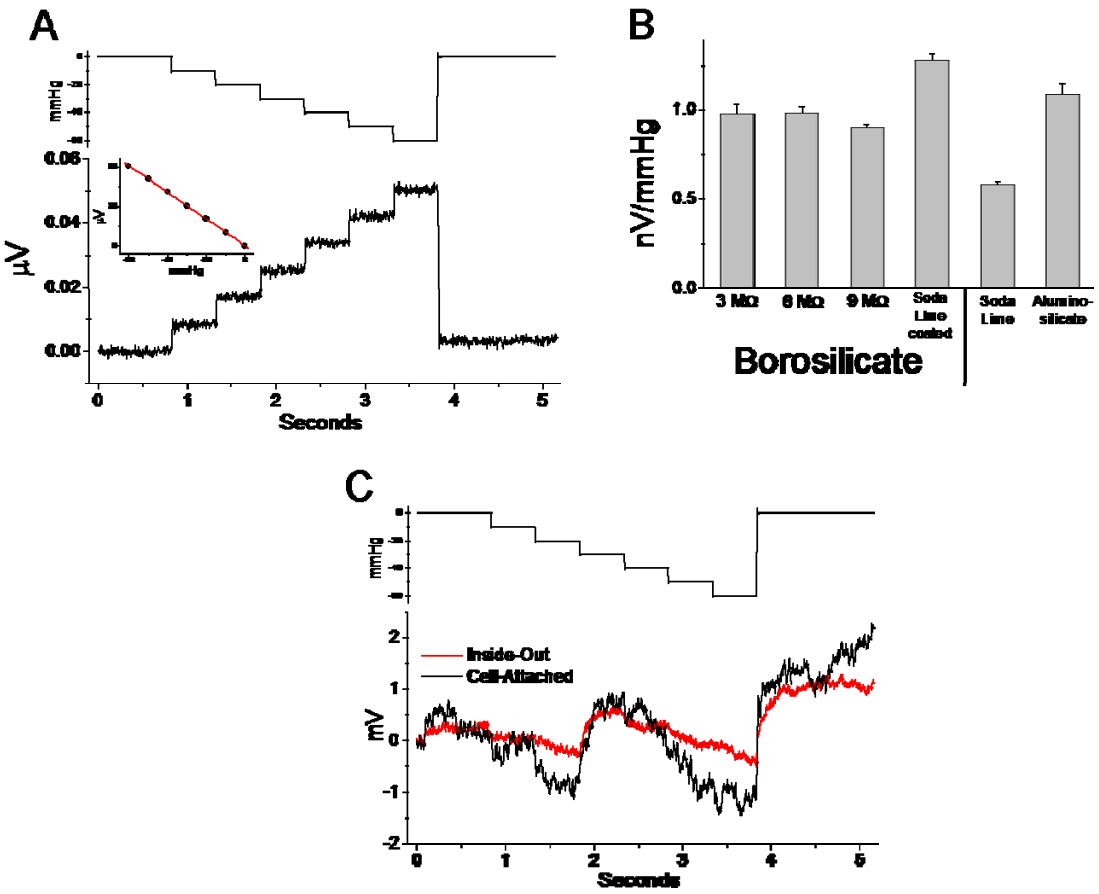


**Figure S6.** Streaming potentials measured in pipettes and patches in current clamp. Negative pressure staircases were applied to open pipettes with symmetrical 140 mM KCl, pH 7 solutions. (A) A typical borosilicate glass pipette (7 MΩ) produced positive streaming potentials with a slope of 0.84 μV/mmHg as shown in the inset. (B) Streaming potential vs. pressure slopes for borosilicate pipettes of different resistance, borosilicate coated with soda lime, soda lime and aluminosilicate glasses of ~7 MΩ (for each value n=4). The test was insensitive to resistance within the range shown. Soda lime had about half the streaming potential as borosilicate indicating that it has about half the surface charge. (C) The average potential changes in cell-attached and inside-out patches (n=5 patches for patch type, average of 10 staircase stimuli for each patch) with resistances between 30-100 GΩ. The voltage changes were unstable probably as a result of changes in patch configuration modifying the seal resistance and the voltage drop produced by the amplifier input current.

**Streaming potentials in a cone and an annulus**

The streaming potential of a shallow cone is:

$$U = \frac{3\varepsilon\,\varepsilon_0 \zeta \Delta P}{2\eta\sigma} * \frac{1 + R_1/R_2}{1 + R_1/R_2 + \left(R_1/R_2\right)^2}$$

where $\zeta$ is the surface potential, $P$ the pressure (133 Pa/mmHg), $\varepsilon\varepsilon_0$ the permittivity ($\varepsilon_0$=8.85*10$^{-12}$ F/m, and $\varepsilon$ is the dielectric constant =80 for water), $\mu$ is the viscosity, $\sigma$ the specific conductivity and $R_1$ and $R_2$ are the pipette radii at the tip and the back. For a long pipette, $R_1/R_2 \rightarrow 0$ and $U \rightarrow \varepsilon\varepsilon_0\zeta\Delta P/2\eta\sigma$. The equation reduces to the familiar Helmholtz-Smoluchowski model for a cylindrical capillary $U = \frac{\varepsilon\,\varepsilon_0 \zeta \Delta P}{\eta\sigma}$ (1). We applied steps of pressure to an empty pipette filled with 100mM KCl ($\sigma$ =1.16 $\Omega^{-1}m^{-1}$) and measured the streaming potential (Fig. 6SA). The slope was -0.84 μV/mmHg (Fig. 6SA insert), and if we assume if $R_1 << R_2$, ε=80, μ=1cp, this suggests ζ=-70mV, close to the value estimated by Gu and Li for neutral borosilicate glass (2). However, glasses having the same name may have different surface potentials depending on the supplier (3).

The cells probably had surface potentials of about -20mV (4) and the gigaseal space is likely to be highly cation selective. If we approximate the seal as a thin conducting annulus with charged walls (the charge is approximated by the mean of the glass and membrane), the streaming potential predicted by a Smoluchowski-Helmholtz calculation is:

$$U_{str} = \frac{\varepsilon\varepsilon_0 \Delta P \zeta}{\eta\sigma} * \frac{1}{4}\left[1 - \frac{2r_D}{h} + \left(1 + \frac{2r_D}{h}\right)\exp\left(-\frac{h}{r_D}\right)\right]$$

where $r_D$ is the Debye length (~ 1nm), $h$ is the thickness of the annulus and the other terms have been previously defined. If $h >> r_D$ $U_{str}$*(annulus)*=1/4 $U_{str}$*(cylinder)* and if $h = r_D$, $U_{str}$*(annulus)*$\rightarrow$*0.025* *$U_{str}$*(cylinder)*. We know from the high resistance of the gigaseal that $h$ cannot be > $r_D$ for normal saline and even if they were equal, the streaming potential would be in the range of nV/mmHg so that we are unlikely to measure the streaming potential of the seal.

Reference List for Streaming Potential


1. Fievet, P., M. Sbai, A. Szymczyk, and A. Vidonne. 2006. Determining the xi-potential of plane membranes from tangential streaming potential measurements: Effect of the membrane body conductance (vol 226, pg 227, 2003). *Journal Of Membrane Science* 281:757.

2. Gu, Y. G. and D. Q. Li. 2000. The zeta-potential of glass surface in contact with aqueous solutions. *Journal of Colloid and Interface Science* 226:328-339.

3. Rae, J. L. and R. A. Levis. 1992. Glass technology for patch clamp electrodes. *Methods Enzymol.* 207:66-92.

4. Zhang, P. C., A. K. Keleshian, and F. Sachs. 2001. Voltage induced membrane movement. *Nature* 413:428-431.

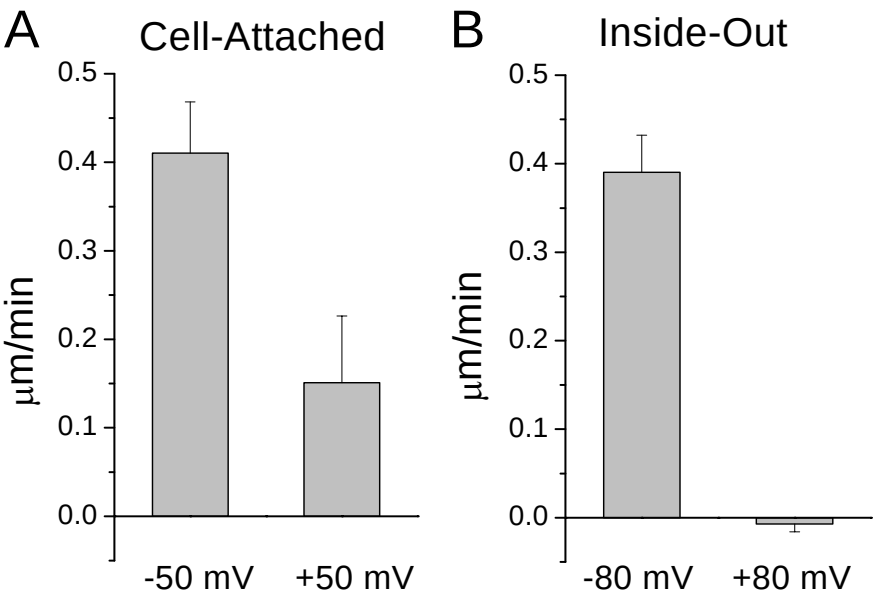


**Figure S7.** Previous studies showed that creep was eliminated when patches were formed in soft glass pipettes (1;2). We measured the surface potential of several glasses using the streaming potential and found soda lime pipettes to have a negative surface charge about half that of borosilicate (see Fig. S6A and B). In soft glass pipettes, patches showed a smooth, voltage-dependent, upward patch creep, although it was significantly slower than observed in borosilicate (A, n = 4). Inside-out patches in soft glass showed an asymmetric voltage dependent creep (B, in symmetrical pH 7, n = 2) similar to pH 5 patches in borosilicate. However, in soft glass the asymmetry of the creep reversed at pH 7. The electroosmosis equations are symmetric in voltage so that reversing polarity should reverse the creep direction. Thus the origin of this asymmetric motion is not clear, but it could be related to the taper of the pipette where subtle geometric asymmetries become pronounced.

Although creep is significantly reduced in soft glass, the voltage dependence remains. However, it should be noted that there are significant differences between the patches in the Gil, et.al. 1999 papers [lead based soft glass (Corning 8161) and membranes from *Xenopus* oocytes] and ours that may account for the complete lack of voltage sensitivity that Gil, et.al. observed.

References

1. Gil, Z., K. L. Magleby, and S. D. Silberberg. 1999. Membrane-pipette interactions underlie delayed voltage activation of mechanosensitive channels in Xenopus oocytes. *Biophys. J.* 76:3118-3127.

2. Gil, Z., S. D. Silberberg, and K. L. Magleby. 1999. Voltage-induced membrane displacement in patch pipettes activates mechanosensitive channels. *Proc Natl. Acad. Sci U. S A* 96:14594-14599.

**Electroosmosis and creep**

Electroosmosis appears to be the force driving voltage dependent patch creep. The fact that the membrane and glass surface charges are negative, substituting larger less mobile cations in the saline slows the rate of voltage dependent creep, and the surface charge can be titrated with pH, all support the idea that the seal space is normally filled with mobile cations. The reversal of voltage-dependent creep direction at pH 5 is consistent with the idea that acidity creates a positively charged space that conducts more anions than cations. The surface potential of borosilicate glass (the $\zeta$ potential) varies from about -40 mV at pH 2 to -80mV at pH 10 (1) and is not likely to be significantly titrated at the pH values we used, suggesting the titrated charges are associated with the membrane.

The factors that are expected to decrease surface charge (i.e., high ionic strength, low pH with negatively charged surfaces and soft glass) cause a decrease in the voltage dependent creep rate. Interestingly, the voltage sensitivity of the creep rate for myotubes was nearly twice that of astrocytes, suggesting the excitable myotube membrane may also have greater surface charge. The use of negative pipette potentials to enhance patch formation can probably be attributed to inwardly directed electroosmosis.

The upper limit of the creep rate is the velocity of water in the seal. That can be estimated from the Helmholtz mobility, $v = \varepsilon\zeta E/\eta$ (2) where $\varepsilon$ is the permittivity (80*8.85 pF/m for water), $\zeta$ is the surface charge (~-50mV), E is the tangential electric field (the applied voltage/seal length) and $\eta$ is the solution viscosity. If we assume E = 50 mV/10 μm = 5,000 V/m, and $\eta$ = 1cP = 0.001 $Ns/m^2$ the water velocity would be 10,620 μm/min, much faster than the measured patch creep of ~1 μm/min. Thus, the creep rate is probably limited by the viscosity of the space which must be much higher than water as suggested by models of the seal resistance (see text and below). If the viscosity of this space increases as $E_a$ increases (compressing the extracellular matrix) that could explain why the voltage sensitivity of the creep rate is pH dependent. As pH decreases, $E_a$ increases, and we expect this to produce greater friction between the glass and the membrane. The creep velocity is a function of the electroosmotic driving force countered by the frictional force created by of $E_a$ and the viscosity of the lipids flowing about proteins immobilized on the glass.

To predict the creep rate as a function of pressure we calculated the velocity for an annular seal capped by a disklike dome (c.f., Fig. S7, and theory below): $V_{creep} = \frac{hR_p \Delta P}{2\eta l}$ where $h$ is the thickness of the seal, $R_p$ is the radius of the pipette; $\Delta P$ is the pressure drop and $\eta$ the viscosity and $l$ the length of the seal. This can be expressed in terms of the seal resistance $R_s = \rho l/2\pi R_p h$ where $\rho$ is the resistivity of the seal media. Combining this with the relationship of mobility to viscosity, $\rho = \rho_0 * \eta / \eta_0$ where $\rho_0$ and $\eta_0$ refer to the adjacent bathing solution, we can express $V_{creep} = \rho_0 \Delta P / \pi R_s$. For 100 mM KCl $\rho_0 = 0.85$ Ωm and for $\Delta P = 10$ mmHg and $R_s = 10$ GΩ , the predicted pressure dependence was $V_{creep} = 2$ μm/min, much faster than we observed (3). Again this argues for the speed being limited by a viscosity within the membrane flowing over immobilized proteins.

## Reference List for Electroosmosis


1. Gu, Y. G. and D. Q. Li. 2000. The zeta-potential of glass surface in contact with aqueous solutions. *Journal of Colloid and Interface Science* 226:328-339.

2. Bockris, J. and A. K. N. Reddy. 1970. Modern Electrochemistry. Plenum Press, New York.

3. Suchyna, T. and F. Sachs. 2007. Mechanical and electrical properties of membranes from dystrophic and normal mouse muscle. *J. Physiol. (Lond)* 581:369-387.

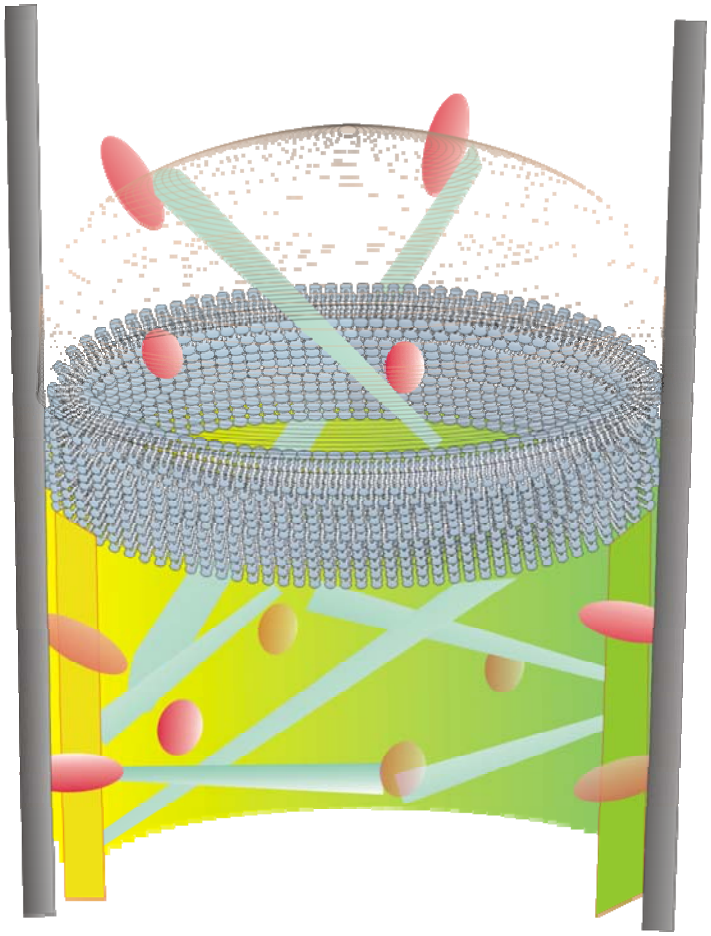

**Figure S8.** A cartoon of a patch that showing the channel free "exclusion band" below the dome that may be the basis of the gigaseal.